

Unoccupied electronic band structure of Na on Cu(111) as studied by inverse photoemission

R. Dudde,* L. S. O. Johansson, and B. Reihl

IBM Research Division, Zurich Research Laboratory, CH-8803 Rüschlikon, Switzerland

(Received 6 November 1990; revised manuscript received 11 February 1991)

We have determined the unoccupied part of the electronic structure of sodium on Cu(111), employing k -resolved inverse photoemission in the isochromat mode. For Na coverages above 0.15 monolayer, an image-potential surface state is observed 2.3 eV above E_F . For the completed $p(2 \times 2)$ Na phase at 0.25-monolayer coverage, a pronounced Na $3p_z$ -derived feature occurs 0.4 eV above E_F , which exhibits a nearly-free-electron-like energy dispersion. For wave vectors $k_{\parallel} \geq 0.6 \text{ \AA}^{-1}$, the unoccupied part of the Na $3s$ band appears close to the Fermi level. We compare our results with recent band-structure calculations for free and adsorbed Na monolayers.

I. INTRODUCTION

The absorption of alkali-metal atoms on metal surfaces has been the subject of numerous experimental and theoretical studies in the past.^{1,2} These studies were motivated by the idea that the alkali-metal-adsorbate system provides an example for a simple chemisorption system. Also the significant promoting properties of alkali metals in heterogeneous catalysis³ have stimulated a number of investigations of the co-adsorption of alkali metals with atoms and molecules on surfaces.⁴ The valence levels of adsorbed alkali-metal atoms can be studied by direct and inverse photoemission, which are both surface-sensitive techniques. In the present study of the Na/Cu(111) system, we continue our recent work of the chemisorption of K on Cu(111).⁵ Since most alkali-metal valence levels that determine the chemical and physical properties are unoccupied, inverse photoemission is particularly powerful for their investigation.

II. EXPERIMENT

The experiments reported below were carried out in a two-chamber ultrahigh-vacuum apparatus.⁶ The base pressures in the spectrometer and in the preparation chambers were in the 10^{-11} -mbar range. The system was equipped with angle-resolved inverse- and ultraviolet-(direct) photoemission spectroscopy (IPS and UPS, respectively), Auger-electron spectroscopy (AES), and low-energy electron diffraction (LEED). The IPS measurements were performed in the isochromat mode, detecting 9.5-eV photons with a Geiger-Müller-type counting tube with a SrF_2 entrance window. The electrostatically focused electron gun⁷ with BaO cathode and the photon detector were mounted at a fixed angle of 30° with respect to each other. The angle of incidence, θ , of the electrons was varied by rotating the sample. The electron-beam divergence was better than 4° , resulting in a resolution of the wave vector k_{\parallel} of $\Delta k_{\parallel} = 0.08 \text{ \AA}^{-1}$. The overall energy resolution (electrons and photons) was 0.35 eV in IPS. Angle-resolved UPS with He I radiation ($h\nu = 21.2 \text{ eV}$) and an overall resolution of 0.1 eV agrees with similar measurements at $h\nu = 4.89 \text{ eV}$ by Lindgren and

Walldén.⁸

The Cu(111) single-crystal surface was cleaned by Ne-ion sputtering and annealing. Its cleanliness was checked by IPS, UPS, and AES. Sodium was evaporated from a commercial getter source (SAES Getters, Italy) onto the sample at room temperature. The pressure during evaporation stayed in the low 10^{-10} -mbar range. The work-function change was determined by the diode method, i.e., by detecting the onset of the absorbed sample current from the electron gun. The coverage-dependent work-function change of the Na/Cu(111) system has been published by Lindgren and Walldén.⁹ In our study we find the same work-function changes with a weak minimum of $\Delta\Phi = -2.3 \text{ eV}$ at a coverage of approximately 0.1 monolayers (ML). We used the occurrence of a clear 2×2 LEED pattern as the calibration point for 0.25 ML of Na coverage. When increasing the coverage above 0.25 ML, we observed a compressed and less sharp hexagonal overlayer structure in LEED.

III. RESULTS AND DISCUSSION

Inverse-photoemission spectra of Na on Cu(111) are presented in Fig. 1 as a function of increasing coverage. The lowermost spectrum shows the normal-incidence IPS curve of the clean Cu(111) surface, where the sharp emission feature at 4.2 eV above the Fermi level represents the image-potential surface states. These states are observed in projected bulk band gaps of metallic surfaces and are fixed in energy relative to the vacuum level.¹⁰ The adsorption of small amounts of Na ($< 0.1 \text{ ML}$) quenches the image-state emission of the clean surface, while a new weaker feature occurs which seems to be connected to the vacuum level (cf. Fig. 1). It will be discussed below. For Na coverages above 0.1 ML, two features emerge in the spectra, which with increasing coverage move to smaller energies, the lower one approaching E_F . Concomitant with the development of these two Na-induced features in IPS, a $p(2 \times 2)$ LEED pattern occurs. For the completed $p(2 \times 2)$ Na phase the two states are located at 0.4 and 2.3 eV above E_F . Heskett *et al.*¹¹ have observed a similar unoccupied two-peak structure in IPS for the Na/Al(111) system, and as-

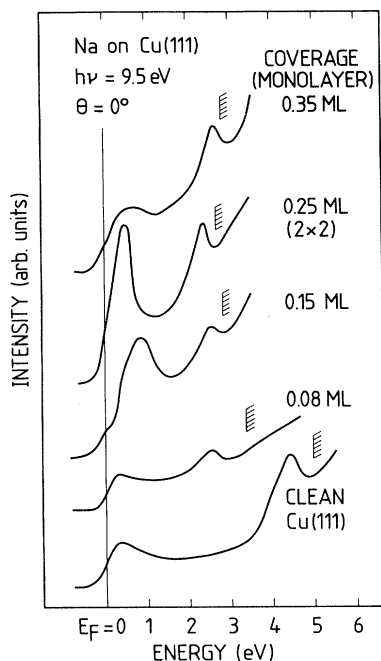


FIG. 1. Normal-incidence inverse-photoemission spectra of Cu(111) at $h\nu=9.5$ eV as a function of Na coverage in monolayers. Note the development of a Na-induced surface state near the Fermi level and the shift of the image-potential state near the vacuum level, which is given by a hatched mark for each spectrum.

signed the lower-lying state to the Na $3p_z$ level. We follow their interpretation, also because this assignment agrees with the band-structure calculation for an isolated sodium monolayer by Wimmer¹² and with a recent model calculation for an adsorbed Na monolayer by Ishida.¹³ In addition, the density-functional calculations by Boettger and Trickey¹⁴ fit this interpretation.

The second, higher-lying state was attributed by Heskett *et al.*¹¹ to a possible contribution from Na d states. However, all calculations^{12–14} reveal only a rather small density of d states at higher energies in the case of sodium. We therefore attribute the emission feature at $E_F+2.3$ eV to an image-potential state of the ordered Na-covered surface. As the work function of the Cu(111)-(2 \times 2)-Na system is reduced to about 2.7 eV, this state is located 0.4 eV below E_{vac} . A similar vacuum-level pinning of the image-state emission with work-function changes as high as in our case ($\Delta\Phi=-2.3$ eV) has been reported for K on Pt(111).¹⁵ This is in contrast to a recent report¹⁰ for K on Cu(100), where the image-state emission follows the work-function change only up to about $\Delta\Phi=-1$ eV. Whether surface order, the exact nature of the projected bulk band gap, or another reason accounts for these different observations is unclear at the moment.

The energy difference between the two unoccupied states of Na on Cu(111) at 0.4 and 2.3 eV in Fig. 1 is 1.9 eV, while on Al(111) we read 1.0 eV for that of the corresponding two-peak structure (cf. Ref. 11). This excludes

an interpretation in terms of intrinsic sodium states for both emission features. However, the variation in the unoccupied electronic structure of Na/Cu(111) and Na/Al(111)¹¹ can easily be explained, if the higher-lying spectral feature reflects an image-potential surface state pinned to the vacuum level rather than band-structure properties of adsorbed sodium. The interpretation as image state also explains the small coverage-dependent energy variations in Fig. 1, which reflect the work-function changes with the amount of adsorbed Na. The identification of image-potential states in adsorbed monolayers of the heavier alkali-metal atoms is less likely to be expected, since for K, Rb, and Cs an increasing density of d states is predicted¹² within the energy range straddling E_{vac} . A possible hybridization of the image states with these d states could prevent the occurrence of such an intense image-state emission as is otherwise observed on metal surfaces with well-defined projected bulk band gaps.⁶

Increasing the sodium coverage beyond the (2 \times 2) phase in Fig. 1 (see the 0.35-ML spectrum) leads to a reduction of the Na p state near E_F , while the image-state emission is not affected. Strong coverage-dependent variations in intensity and energy have been reported^{11,16} for alkali-metal valence-band emission as measured by UPS. We attribute the p -band intensity reduction at coverages above 0.25 ML in Fig. 1 to an energetic broadening of this state due to an increasing disorder in the Na adlayer when going beyond the (2 \times 2) phase. However, we also want to note here the observation¹⁷ of an anomalous peak near E_F in UPS of Na(110), as well as the disappearance with coverage¹⁸ of a narrow peak just below E_F for Na/Cu(111), which Lindgren and Walldén have interpreted¹⁸ as part of a series of discrete potential-barrier states, i.e., modified image-potential states, where the lowest unoccupied state should occur¹⁸ at $E_F+2.25$ eV in very good agreement with our observation of the image-state emission in Fig. 1 (see the discussion above).

There is a downward shift of the Na $3p$ emission in Fig. 1 when going from 0.15 to 0.25 ML coverage. This shift is similarly observed for the Na p emission of the Na/Al(111) system¹⁶ and reflects the depolarization effect,^{19–21} i.e., the increasing electrostatic field at the surface, which causes the strong reduction of the work function.

Next we applied angle-resolved IPS to the (2 \times 2) Na phase on Cu(111) to obtain the two-dimensional energy-band dispersion. Corresponding inverse-photoemission spectra are presented in Fig. 2 as a function of polar angle θ along the $\bar{\Gamma}-\bar{M}$ azimuth of the surface Brillouin zone. We note an upward dispersion of the two intense emission features of Fig. 1 just discussed above. The image-state emission can be followed only up to $\theta=15^\circ$ and exhibits a similar upward dispersion along along the $\bar{\Gamma}-\bar{K}$ azimuthal direction in Fig. 3. Turning now to the Na p emission, we observe a strong dispersion from the Fermi level at normal incidence up to 2.1 eV at $\theta=32.5^\circ$ in Fig. 2, resulting in a total bandwidth of 1.7 eV. At 27.5° a new intense emission feature emerges near E_F which exhibits a weaker upward dispersion with increasing θ (cf. Fig. 2). We attribute this band to the unoccu-

pied part of the Na $3s$ band that is expected¹²⁻¹⁴ to turn up from the occupied region and cross the Fermi level along $\bar{\Gamma}-\bar{K}$ and $\bar{\Gamma}-\bar{M}$. For a discussion of the various band dispersions, we have plotted the peak positions of all spectral features of Figs. 2 and 3 as a function of k_{\parallel} in Fig. 4. Also included in Fig. 4 is the $\theta=0^{\circ}$ UPS value of the occupied s band measured with $h\nu=21.2$ eV, which disappeared for $\theta \geq |2.5^{\circ}|$ (original spectra not shown). We note a similar dispersion behavior for both the Na p state as well as the image-potential state along the $\bar{\Gamma}-\bar{K}$ and $\bar{\Gamma}-\bar{M}$ directions. The Na s band occurs at polar angles of 27.5° in Fig. 2 and 25° in Fig. 3, respectively, corresponding roughly to $k_{\parallel}=0.6 \text{ \AA}^{-1}$. A possible interpretation in terms of copper bulk bands can be ruled out by comparing to the elaborate IPS work on bulk transitions by Schneider *et al.*²² for Cu(111).

We have found significant Na $3s$ emission intensity only around the \bar{M} and \bar{K} points. It is known, however, that the limited energy and k_{\parallel} resolution in UPS and IPS prevents an exact determination of the Fermi-level crossing.²³ For the s band we therefore expect it to occur at smaller k_{\parallel} values, as also suggested by calculations¹² for the hexagonal monolayer, where the s band crosses at about $\frac{2}{3}$ between the $\bar{\Gamma}$ and \bar{K} points. Along the $\bar{\Gamma}-\bar{K}$ symmetry direction it exhibits¹² strong upward disper-

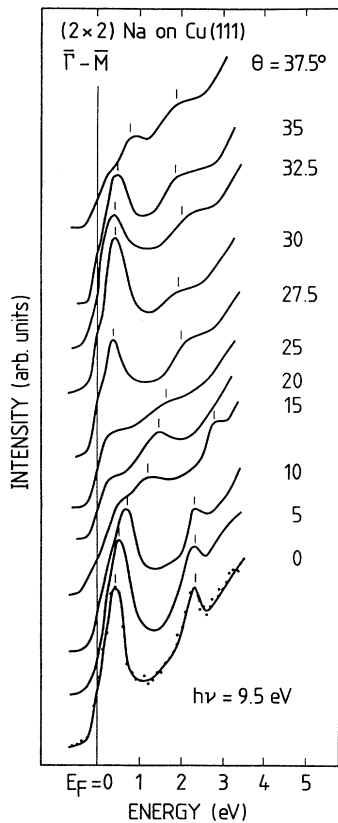


FIG. 2. Angle-resolved inverse-photoemission spectra at $h\nu=9.5$ eV for different incidence angles θ , probing states along the $\bar{\Gamma}-\bar{M}$ line of the Cu(111)-(2 \times 2)-Na surface Brillouin zone.

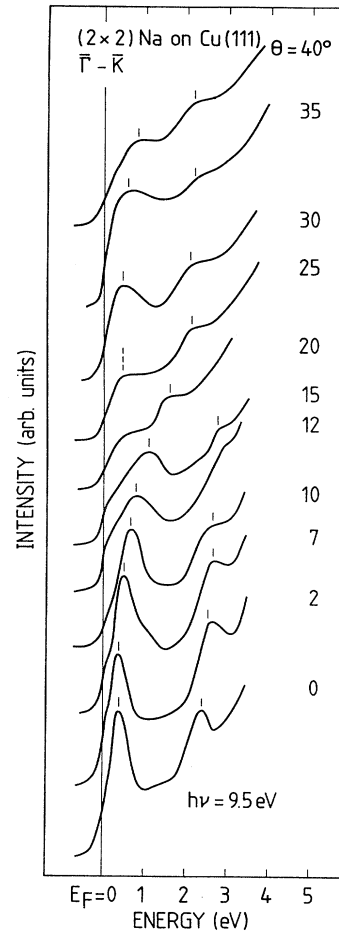


FIG. 3. Angle-resolved inverse-photoemission spectra at $h\nu=9.5$ eV for different incidence angles θ , probing states along the $\bar{\Gamma}-\bar{K}$ line of the Cu(111)-(2 \times 2)-Na surface Brillouin zone.

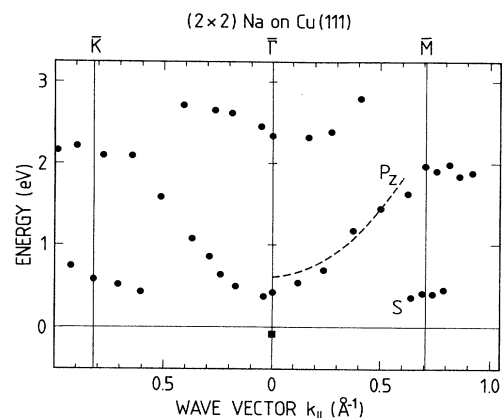


FIG. 4. Energy dispersion $E(k_{\parallel})$ of the surface-state features as derived from Figs. 2 and 3 (solid dots). The solid square denotes the $\theta=0^{\circ}$ UPS value of the occupied s band measured with $h\nu=21.2$ eV photons (original spectra not shown). The dashed line represents the calculated center of gravity of the Na $3p_z$ band for a Na overlayer on semi-infinite jellium (from Ref. 13).

sion, while we find only a weak dispersion in Fig. 4. Again, the actual dispersion behavior of the spectral features may be obscured by their proximity to E_F .

In his local-density functional theory for the electronic structure of an isolated sodium monolayer, Wimmer¹² used a nearest-neighbor spacing of 2.66 Å. This small Na-Na distance causes the calculated dispersion to be much stronger than the dispersion measured here for a 2×2 Na overlayer with a Na-Na distance of 5.11 Å. Bearing this in mind, we at least qualitatively find agreement between our results of Fig. 4 and Wimmer's calculated electronic structure. In particular, the predicted p_z band starting at about $E_F + 0.6$ eV at $\bar{\Gamma}$ exhibits the correct strong upward dispersion.

In his calculations Ishida¹³ has tried to simulate Na adsorbed on Al(111) by a Na overlayer on semi-infinite jellium. Ishida's results show good agreement with the occupied part of the 4s band of K on Al(111) as determined by Horn *et al.*²⁴ Also from this calculation, $3p_z$ character has to be assigned by the measured Na band, and we have plotted the calculated¹³ center of gravity of the Na $3p_z$ band as a dashed line along the $\bar{\Gamma}-\bar{M}$ azimuth in Fig. 4. It is expected¹³ to form a rather broad structure. In our study the observed sharp p emission at $\bar{\Gamma}$ in Figs. 2 and 3 has a full width at half maximum of 0.4 eV and is solely determined by the experimental energy resolution. Hence the intrinsic width of the p_z at $\bar{\Gamma}$ must be smaller than 150 meV.

In the calculations of Boettger and Trickey,¹⁴ local-

density-functional theory is used to obtain the equilibrium lattice parameters and the electronic structure for hexagonal monolayers of the alkali metals and alkaline-earth metals. For a comparison with our experiment, it is again clear that the calculated energy dispersion is too strong as the Na-Na distance is much smaller in the hexagonal monolayer than in the 2×2 overlayer phase we studied. Hence, as with Wimmer's calculation¹² discussed above, agreement between theory and experiment can only be found in a qualitative manner.

In summary, we have studied the unoccupied electronic structure of Na on Cu(111) by inverse photoemission. At coverages below 0.25 ML a Na $3p$ -derived state is observed which shifts with increasing coverage towards the Fermi level. This coverage-dependent shift is in agreement with the results for the adsorption of K on Ag(110)²⁵ and alkali-metal atoms on Al(111).¹⁶ At 0.25 ML an ordered $p(2 \times 2)$ Na overlayer is formed that exhibits a sharp Na $3p_z$ state 0.4 eV above E_F and an image-potential state which is pinned by the vacuum level $E_{\text{vac}} = E_F + 2.7$ eV. The unoccupied Na $3s$ band can only be discerned around the \bar{M} and \bar{K} points. The measured band dispersion of all Na-induced states compares rather well with Ishida's calculation¹³ for a Na monolayer on semi-infinite jellium.

ACKNOWLEDGMENT

We thank M. Tschudy for his competent assistance.

*Present address: Fraunhofer Institut für Mikrostrukturtechnik, Margarete-Steiff-Weg 3, D-2210 Itzehoe, Federal Republic of Germany.

¹E. G. Bauer, in *The Chemical Physics of Solid Surfaces and Heterogeneous Catalysis*, edited by D. A. King and D. P. Woodruff (Elsevier, New York, 1983), Vol. 3B.

²H. P. Bonzel, *J. Vac. Sci. Technol. A* **2**, 866 (1984), and references cited therein.

³W.-D. Mross, *Catal. Rev. Sci. Eng.* **25**, 591 (1983).

⁴P. J. Feibelman and D. R. Hamann, *Surf. Sci.* **149**, 48 (1985).

⁵R. Dudde, K. H. Frank, and B. Reihl, *Phys. Rev. B* **41**, 4897 (1990).

⁶B. Reihl, *Surf. Sci.* **162**, 1 (1986).

⁷P. W. Erdman and E. C. Zipf, *Rev. Sci. Instrum.* **53**, 235 (1982).

⁸S. Å. Lindgren and L. Walldén, *Phys. Rev. Lett.* **59**, 3003 (1987).

⁹S. Å. Lindgren and L. Walldén, *Phys. Rev. B* **22**, 5967 (1980).

¹⁰See the discussion by D. P. Woodruff and N. V. Smith, *Phys. Rev. B* **41**, 8150 (1990).

¹¹D. Heskett, K. H. Frank, E. E. Koch, and H. J. Freund, *Phys. Rev. B* **36**, 1276 (1987).

¹²E. Wimmer, *J. Phys. F* **13**, 2313 (1983).

¹³H. Ishida, *Phys. Rev. B* **40**, 1341 (1989).

¹⁴J. C. Boettger and S. B. Trickey, *J. Phys. Condens. Matter* **1**, 4323 (1989).

¹⁵A. Goldmann, V. Dose, and G. Borstel, *Phys. Rev. B* **32**, 1971 (1985).

¹⁶K. H. Frank, H. J. Sagner, and D. Heskett, *Phys. Rev. B* **40**, 2767 (1985).

¹⁷E. Jensen and E. W. Plummer, *Phys. Rev. Lett.* **55**, 1912 (1985).

¹⁸S. Å. Lindgren and L. Walldén, *Phys. Rev. B* **38**, 3060 (1988).

¹⁹R. W. Gurney, *Phys. Rev.* **47**, 479 (1935).

²⁰N. D. Lang, *Phys. Rev. B* **4**, 4234 (1971); N. D. Lang and A. R. Williams, *ibid.* **18**, 616 (1978).

²¹J. P. Muscat and D. M. Newns, *Surf. Sci.* **74**, 355 (1978); **84**, 262 (1979).

²²R. Schneider, H. Dürr, Th. Fauster, and V. Dose, *Phys. Rev. B* **42**, 1638 (1990).

²³R. Clauberg, K. H. Frank, J. M. Nicholls, and B. Reihl, *Surf. Sci.* **189/190**, 44 (1987).

²⁴K. Horn, A. Hohlfeld, J. Somers, Th. Lindner, P. Hollins, and A. M. Bradshaw, *Phys. Rev. Lett.* **61**, 2488 (1988).

²⁵W. Jacob, E. Bertel, and V. Dose, *Phys. Rev. B* **35**, 5910 (1987).